AIMS Materials Science, 4(3): 670-679.
DOI: 10.3934/matersci.2017.3.670
Received: 22 March 2017
Accepted: 21 May 2017
Published: 26 May 2017

http://www.aimspress.com/journal/Materials

Research article

New DC conductivity spectra of Zn–Al layered double hydroxide (Zn–Al–NO_3–LDH) and its calcined product of ZnO phase

Abdullah Ahmed Ali Ahmed [1,*], Zainal Abidin Talib [2], Mohd Zobir Hussein [3], and Yusra Abdullah Ahmed Al-Magdashi [1]

[1] Department of Physics, Faculty of Applied Science, Thamar University, Dhamar 87246, Yemen
[2] Department of Physics, Faculty of Science, Universiti Putra Malaysia, 43400 UPM Serdang, Selangor, Malaysia
[3] Advanced Materials and Nanotechnology Laboratory, Institute of Advanced Technology (ITMA), Universiti Putra Malaysia, 43400 UPM Serdang, Selangor, Malaysia

* **Correspondence:** Email: abdullah2803@gmail.com; Tel: +967771792950.

Abstract: Zn–Al–NO_3–LDH nanostructure was synthesized via the coprecipitation method at molar ratio Zn^{2+}/Al^{3+} = 4 and pH = 7. The resultant sample was thermally treated at calcined temperatures of 50, 100, 150, 200, 250 and 300 ℃. The layered structure of the Zn–Al–NO_3–LDH samples was stable below the calcination temperature 200 ℃ as shown in powder X-ray diffraction (PXRD) patterns of calcined samples. The calcination products showed a collapse of LDH structure and ZnO phase was formed at 200 ℃ and above. The dielectric spectroscopy of LDH was explained using anomalous low frequency dispersion (ALFD) due to the low mobility of LDH carriers. The conductivity spectra of LDH can be theoretically described according to the effective phase within the calcination products of LDH. In the comparison with previously researches, this study presented higher values of DC conductivity for all studied samples.

Keywords: layered double hydroxide nanostructure; ZnO; co-precipitation method; heat treatment; DC conductivity; anomalous low frequency dispersion

1. Introduction

The kind of layered double hydroxides (LDHs) components are anionic clays and have a flat two-dimensional layered structure. The structures of LDH layers has positively charged brucite [(M^{II}, M^{III})$(OH)_x$]-like layers where (M^{II}) and (M^{III}) are trivalent and divalent cations, respectively. The brucite layers have (M^{II}) and (M^{III}) cations in their octahedral center (OH^-). The interlayer galleries were occupied by A^{n-} anions and water molecules to balance the resulting brucite layers. The chemical composition of LDH was described by the formula $[M^{II}_{1-x}M^{III}_x(OH)_2]^{x+}$ $\{(A^{n-}_{x/n})\ mH_2O]^{x-}$, where n is the anion charge. The coefficient x is the same amount as the molar ratio $[M^{III}/(M^{II} + M^{III})]$, and m is the number of water molecules presented in the region of interlayer [1].

The importance of LDH materials rose from their ability to intercalate anionic compounds into LDH interlayers. This property makes LDHs useful for the removal of NO_x and SO_x from flue gas combustion and the purification of water by removing microorganisms (such as bacteria and viruses). This property also allowed LDHs to be used as catalysis and for drug and gene delivery [2–6].

LDHs have low mobility charge carriers which are believed to be responsible for the dielectric response.

Zn–Al–NO_3–LDH has two charge carriers (proton of water clusters and nitrate ions in the LDH interlayer). For that, LDHs have low mobility charge carriers. The anomalous low frequency dispersion (ALFD) has been used to describe the dielectric behavior for the pristine layered double hydroxide [7].

Ivanov et al. [8] have been studied the dielectric and conductive properties of layered double hydroxide compound in frequency range of (20 Hz–1 MHz) for two kinds of samples, wet and dry samples. This study was carried out at different temperature values (30–290 K) and (160–290 K) for dry and wet samples, respectively. The DC conductivity values for all studied samples were found below 10^{-5} S/m and it increased as temperature increased in range of (250–290 K) [8]. In the materials of the layered double hydroxide (Ni–Al–Mo_7O_{24}–LDH and Zn–Al–Mo_7O_{24}–LDH), the dielectric relaxation originated from the reorientational functions of water molecules adsorbed on the oxide surface or in the interlayer regions [9]. As seen in our observations [10], the measurements of the Zn–Al–NO_3–LDH in situ dielectric at temperature below 100 ℃ (27, 50, 70 and 90 ℃) were described by ALFD using the second type of Universal Power. The DC conductivity of LDH increased as the in situ temperature increased.

In this work, the nanostructure of molar ratio of Zn–Al–NO_3–LDH at Zn^{2+}/Al^{3+} = 4 and at constant pH = 7 has been prepared using method of co-precipitation. The LDH was calcined at 50, 100, 150, 200, 250 and 300 ℃. PXRD was used to study the structural properties of the synthesized samples. At several calcined temperatures the Dielectric measurements of the Zn–Al–NO_3–LDH were also recorded.

2. Materials and Method

2.1. Materials

The zinc nitrate starting chemicals ($Zn(NO_3)_2$ $6H_2O$) (Systerm, 98%), aluminum nitrate ($Al(NO_3)_3$ $9H_2O$) (Hamburg Chemicals Co., 99.4%) and sodium hydroxide (NaOH) (Merck Co.,

99%) were used without further purification. Deionized water was used as solvent throughout this study.

2.2. Preparation of Samples

The Zn–Al–NO_3–LDH precursors preparation has been carried out using co-precipitation method with molar ratios of Zn^{2+}/Al^{3+} = 4. The slow addition was used to carry out the synthesis of two metal nitrate solutions, and [0.1 mol L^{-1} of $Zn(NO_3)_2$ $6H_2O$], under constant stirring. The solution was prepared at pH = 7 by the dropwise addition of aqueous NaOH (1.0 mol L^{-1}). The titration of NaOH was conducted beneath a stable flow of nitrogen gas to invalidate (leastways minimise) contamination by atmospheric CO_2. The slurry results were presented at 70 ℃ on account of 18 h with the shaker of an oil bath (70 rpm). The deionised water was used to wash the precipitate by centrifugation for a number of times and dehydrated in an oven at 70 ℃ on account of 48 hours. The nanocomposite results were ground into a smooth powder and stored in bottles of sample for additional use.

Heat-treated samples of Zn–Al–NO_3–LDH were prepared by heating the LDH at 50, 100, 150, 200, 250 and 300 ℃. The samples are labelled as Zn–Al–LDH–*T*, where *T* represents the calcination temperature. The heating was performed in an electric tubular furnace at atmospheric pressure in a ceramic boat for 5 h. When the heat treatment was completed, the sample was allowed to cool to room temperature and kept in a sample bottle for further characterisation [11].

2.3. Characterization

PXRD patterns of the samples were obtained on a X-ray diffractometer (X'PERT-PRO PANALYTICAL) using CuK_α (λ = 1.54187 Å) radiation at 40 kV and 30 mA. Novocontrol high resolution dielectric analyzer has been used to measure the dielectric relaxations of the samples.

3. Results and Discussion

3.1. The Study of Powder X-ray Diffraction

Figure 1 exhibits 3D plots PXRD patterns intensity, 2theta and calcination temperature of samples. Figure 1a shows PXRD patterns which are the characteristic reflections of the Zn–Al–NO_3–LDH structure at the planes of (003), (006), (009), (101), (110) and (113) [12]. PXRD patterns in Figure 1a also exhibits that LDHs structure was not affected when it was calcined at 150 ℃ and below. The lattice parameter values for Zn–Al–NO_3–LDH are recorded in Table 1. The ZnO phase with low intensity was present within LDH samples in this range of calcined temperatures.

As seen in Table 1, the decrease in value of the unit cell parameter *c* indicates to the decrease in the interlayer thickness as the calcined temperature increases. This is due to the liberation of water molecules from the interlayer gallery [13].

However, increasing of the calcined temperature above 200 ℃ caused the collapse of the layered structure of LDH and at the same time the emergence of ZnO phase as shown in Figure 1b. PXRD patterns of ZnO phase is indicated by peaks at 2θ = 31.8°, 34.5°, 36.3°, 47.6°, 56.6°, 62.9°, 66.4°, 68° and 69.1°, corresponding to the reflections from (100), (002), (101), (102), (110), (103),

(200), (112) and (201) planes, respectively [14]. The intensity of ZnO patterns increases as the increasing of the calcined temperature [13,15], which indicates the increase in the crystallinity of ZnO phase.

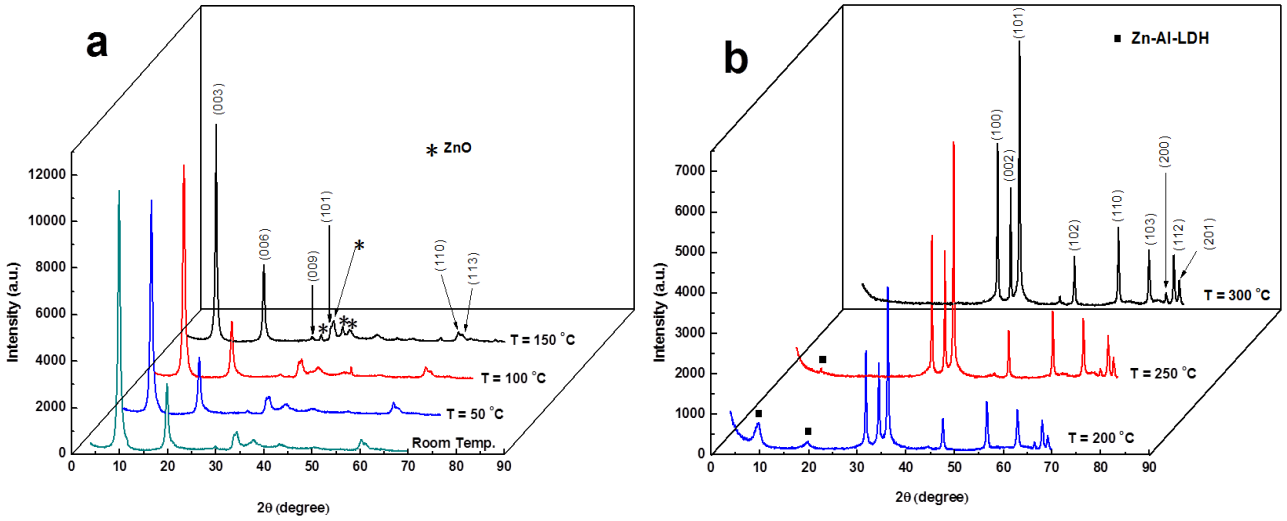

Figure 1. PXRD patterns of (a) Zn–Al–LDH before thermal treatment and Zn–Al–LDH at calcined temperature range of 50, 100 and 150 ℃, with (*) ZnO phase. (b) Zn–Al–LDH at calcined temperatures of 200, 250 and 300 ℃. The small black square represents the LDH phase after calcination above 150 ℃.

Table 1. The calculated unit cell parameters and the textural features for Zn–Al–NO_3–LDH samples.

Sample	d_{003} (nm)	d_{110} (nm)	a [a] (nm)	c [b] (nm)	D [c] (nm)	$h_{inter.}$ [d] (nm)
Zn–Al–LDH	0.892	0.154	0.308	2.684	19.85	4.15
Zn–Al–LDH-50 ℃	0.892	0.154	0.308	2.683	18.56	4.14
Zn–Al–LDH-100 ℃	0.887	0.154	0.308	2.679	22.13	4.13
Zn–Al–LDH-150 ℃	0.887	0.153	0.306	2.670	22.75	4.10

[a] $a = 2d_{110}$; [b] $c = (3d_{003} + 6d_{006} + 9d_{009})/3$; [c] Average crystallite size in c direction: calculated from the values of (003), (006) and (009) diffraction peaks using the Scherrer equation; [d] $h_{inter.}$ = the interlayer thickness = (c/3 – brucite-like sheet thickness).

3.2. Conductivity Spectra

LDH materials have two types of charge carrier which are responsible for the dielectric relaxation [7]. As reported in our earlier article [11], the proton of the polarized clusters of water is the first carrier and the nitrate ions of the interlayer LDH region is the second one. The proton transfers to produce OH^- and OH_3^+ ions at every path end of water clusters in the presence of the applied electric field due to proton hopping (intercluster hopping at low frequency region and

intracluster hopping at high values of frequency). In this condition, nitrate ions also transfer from their equilibrium positions to serve as an additional charge carrier.

The real part's results of the conductivity $\sigma'(\omega)$ spectra of prepared and calcined LDH samples were also reported as shown in Figures 2 and 3. Figure 2 represents the results for samples of the normal structure of LDH which were calcined at temperature of 150 ℃ and below, while Figure 3 represents ZnO phase due to the collapse of LDH structure at calcined temperature of 200, 250 and 300 ℃.

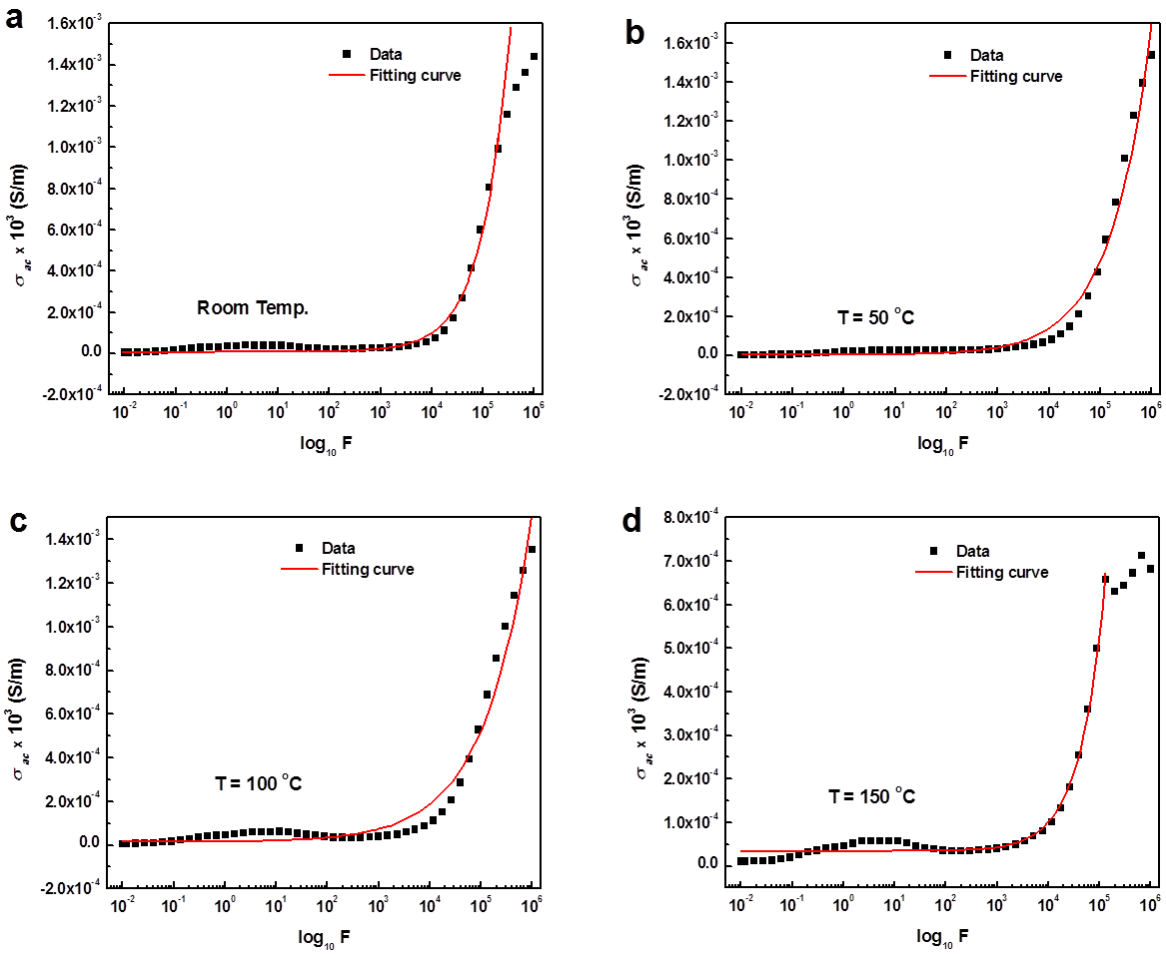

Figure 2. Frequency dependence of real part of conductivity σ' in the room temperature (a) and at different calcined temperatures of (b) 50 ℃, (c) 100 ℃ and (d) 150 ℃. The continuous solid line in σ' spectra represents the fit of experimental data of the Jonscher power law (equation 1).

Figure 2 shows that $\sigma'(\omega)$ becomes almost independent of frequency below a certain value when it decreases with decreasing of the frequency. The ionic or DC conductivity (σ_{DC}) will be obtained by extrapolation of this part of spectra towards lower frequency.

According to ALFD, the behavior of $\sigma'(\omega)$ spectra follows the Jonscher power law [16] which is given by Eqn. (1) and the fitting is illustrated in Figure 2:

$$\boldsymbol{\sigma_{ac}(\omega) = \sigma_{DC} + A\omega^{n}} \quad (1)$$

In Eqn. (1), $\boldsymbol{\sigma'(\omega) = A\omega^n}$ represents "true ac conductivity" and $\boldsymbol{A}$ is the factor of pre-exponential and $\boldsymbol{n}$ is the range of fractional exponent between 0 and 1 for this material [17]. The fit of the experimental data to power law expression is shown by The solid line in the $\sigma'(\omega)$ spectra denotes. The fit values of the DC conductivity σ_{DC}, A and n were obtained using Origin® nonlinear curve fitting software and recorded in Table 2. As seen in previous literature [8], the DC conductivity values were found in range of (10^{-6}–~10^{-8} S/m), while values were found in this study exhibited higher contribution (~10^{-3} S/m) as listed in Table 2.

Table 2. Values of DC conductivity σ_{DC}, pre-exponential factor A and the fractional exponent n for fresh Zn–Al–NO_3–LDH sample and calcined LDH samples at 50, 100 and 150 ℃.

Sample	$\sigma_{DC} \times 10^{-3}$ (S/m)	$A \times 10^{-7}$	n
Zn–Al–LDH	4.49	0.48	0.82
Zn–Al–LDH-50 ℃	3.13	9.00	0.55
Zn–Al–LDH-100 ℃	13.79	23.36	0.47
Zn–Al–LDH-150 ℃	34.59	2.01	0.88

As previously mentioned, Table 2 shows new σ_{DC} values of the Zn–Al–NO_3–LDH structure for the range of the calcination temperatures and σ_{DC} increases as the calcined temperature increases. This phenomenon is due to the interlayer distance, water content [18], anion in LDH interlayer and relative humidity [19,20]. The loss of molecules of water from the LDH interlayer with increasing of the temperature results in the decrease in interlayer distance which implies anion (nitrate ion) conductivity decreases as interlayer distance decreases [18]. As seen in Table 1, the interlayer thickness decreased slightly while, water content decrease rapidly as calcined temperature increases in this range of temperature as reported in our work [11]. This suggests that the increasing of calcined temperature as a result of the increasing of the removal of water which allows the increasing in the ionic conductivity because the very low electrical conductivity of the water molecule. Light et al. [21], who stated that the sensitivity of pure water conductivity changed in temperature, confirm our suggestion. Fourier transform infrared (FT-IR) and the electron spin resonance (ESR) spectra exhibit the presence of nitrate anions with D_{3h} symmetry in LDH interlayer as seen in our observations [11,22]; consequently the nitrate anion has a process based transport. This symmetry may give the nature of the ion transport mainly responsible for the measured conductivity [23]. The ionic conductivity increases as the calcined temperature increases at range below the decomposition point (460 ℃).

The conductivity spectra for calcined samples at 200, 250 and 300 ℃ are shown in Figure 3. As seen in Figure 2, Figure 3 shows $\sigma'(\omega)$ indicates the decrease with the decreasing of frequency and becomes independent of frequency below a certain value.

Tripathi et al. [24] have shown that the ac conductivity of pure ZnO phase was increasing function of frequency. The real part $\sigma'(\omega)$ spectra can be explained using the power law defined as [16,25]:

$$\boldsymbol{\sigma'(\omega) = \sigma_{DC}\left[1 + \left(\frac{\omega}{\omega_c}\right)^n\right]} \quad (2)$$

where $\boldsymbol{\omega_c}$ is the hopping frequency of the charge carriers and $\boldsymbol{n}$ is the dimensionless frequency exponent ranging between 0 and 1. The experimental conductivity spectra of ZnO are fitted to Eqn. (2). The solid line in the $\sigma'(\omega)$ spectra denotes the fitting data to power law expression and the fit values of the DC conductivity σ_{DC}, ω_c, A and n were obtained using Origin® nonlinear curve fitting software and listed in Table 3. The DC conductivity values of studied samples regarding to ZnO phase were found with higher values than that obtained by this literature [24], which were below $\sim 10^{-5}$ S/m.

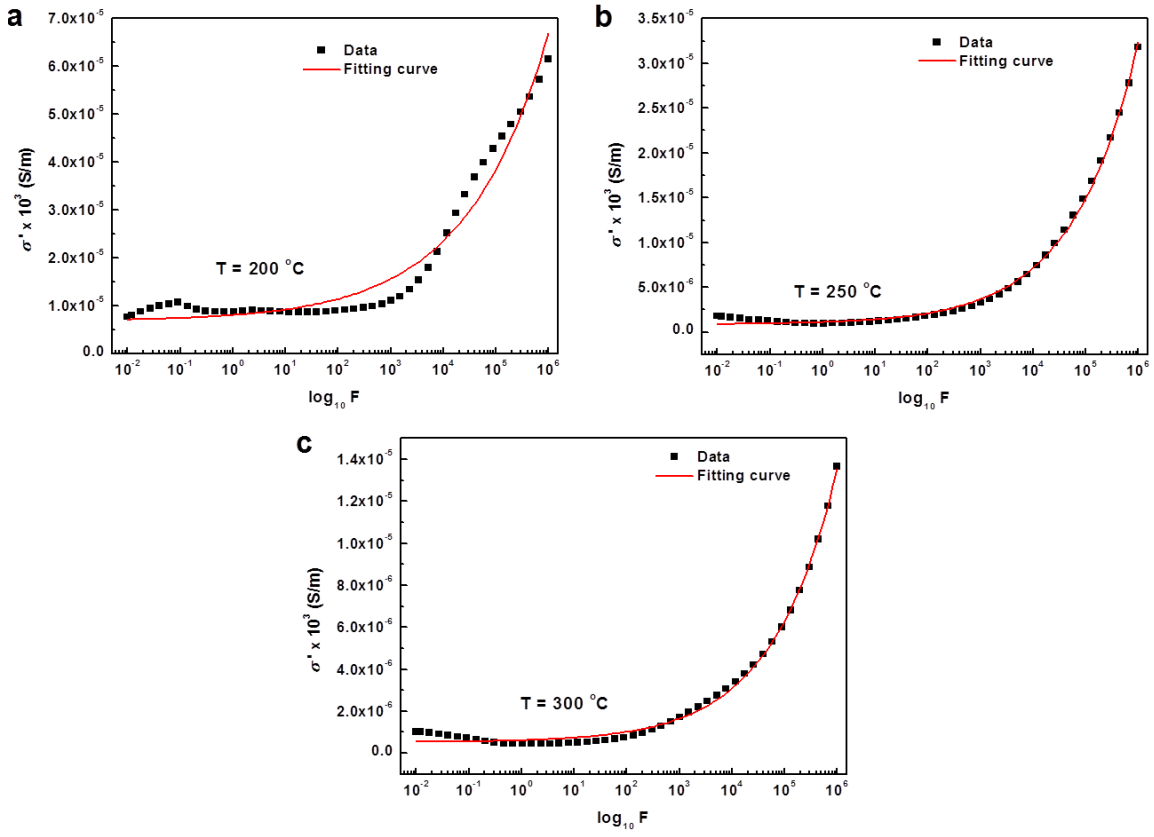

Figure 3. Frequency dependence of real part of conductivity σ' at different calcined temperatures of (a) 200 ℃, (b) 250 ℃ and (d) 300 ℃. The continuous solid line in σ' spectra represents the fit of experimental data of the Jonscher power law (equation 2).

Table 3. Values of DC conductivity σ_{DC}, hopping frequency ω_c and the fractional exponent n for calcined Zn–Al–NO_3–LDH at 200, 250 and 300 ℃.

Sample	$\sigma_{DC} \times 10^{-3}$ (S/m)	ω_c (Hz)	n
Zn–Al–LDH-200 ℃	6.75	377.36	0.28
Zn–Al–LDH-250 ℃	0.85	31.58	0.35
Zn–Al–LDH-300 ℃	0.51	103	0.35

Normally, the σ_{DC} spectra of ZnO increases as calcined temperature increases [26] due to the existence of a conductive process in ZnO, while σ_{DC} values in our results (Table 3) decrease as calcined temperature increases. This observation can be referred to the presence of ZnO with other

phase which forms in the calcination process such as residues of LDH (as shown in Figure 1b with temperatures 200 and 250 ℃) and aluminum hydroxide oxide AlO(OH) [12]. The presence of aluminum hydroxide oxide allows decreasing of σ_{DC} value due to the insulating effect of this material.

In the calcined sample at 200 ℃, the fit curve shows some disagreement with experimental data due to this sample still clearly contains LDH phase (Figure 1b, which marked within black square symbol). This makes it as intermediate sample between LDH structure and collapsed structure of LDH.

4. Conclusions

The structure of Zn–Al–NO_3–LDH was stable at calcined temperatures between 50 and 150 ℃. At calcined temperatures of 200 ℃ and above, the new stage of ZnO was formed and the LDH structure collapsed. The dielectric behavior of LDH samples can be explained by the ALFD which is modeled by the Universal Power Law (second type). Results of all the samples show that the real part of conductivity becomes almost independent of frequency below a certain value and decreases with the decreasing frequency. The ionic or DC conductivity (σ_{DC}) will be given by the prediction of this part of spectra towards lower frequency, which obtained new values in range of $\sim 10^{-3}$ S/m. The DC conductivity of calcined LDH blow the temperature of 200 ℃ increased according to the elimination of the water molecules and the existence of nitrate anions in LDH interlayer. On the other hand, the DC conductivity of the calcined samples at 200 ℃ and above decreased with the increase in temperature due to the presence of ZnO with calcination products.

Acknowledgments

This study was financed by Universiti Putra Malaysia (UPM) for supporting this work.

Conflict of Interests

The authors declare that they have no conflict of interests in this work.

References

1. Cavani F, Trifirò F, Vaccari A (1991) Hydrotalcite-type anionic clays: preparation, properties and applications. *Catal Today* 11: 173–301.
2. Braterman PS, Xu ZP, Yarberry F (2004) Layered Double Hydroxides (LDHs). In: Auerbach SM, Carrado KA, Dutta PK, *Handbook of layered materials*, New York: Marcel Dekker Inc., 373–474.
3. Jin S, Fallgren PH, Morris JM, et al. (2007) Removal of bacteria and viruses from waters using layered double hydroxide nanocomposites. *Sci Technol Adv Mat* 8: 67–70.
4. Li SP, Hou WG, Hu JF, et al. (2003) Influence of shear rate on thixotropic suspensions. *J Disper Sci Technol* 24: 709–714.
5. Tamura H, Chiba J, Ito M, et al. (2004) Synthesis and characterization of hydrotalcite-ATP intercalates. *Solid State Ionics* 172: 607–609.

6. Williams GR, O'Hare D (2006) Towards understanding, control and application of layered double hydroxide chemistry. *J Mater Chem* 16: 3065–3074.
7. Mehrotra V, Giannelis EP (1992) On the dielectric response of complex layered oxides: Mica-type silicates and layered double hydroxides. *J Appl Phys* 72: 1039–1048.
8. Ivanov M, Klemkaite K, Khinsky A, et al. (2011) Dielectric and Conductive Properties of Hydrotalcite. *Ferroelectrics* 417: 136–142.
9. Frunza L, Schönhals A, Frunza S, et al. (2007) Rotational fluctuations of water confined to layered oxide materials: Nonmonotonous temperature dependence of relaxation times. *J Phys Chem A* 111: 5166–5175.
10. Ahmed AAA, Talib ZA, Hussein MZB, et al. (2012) In situ dielectric measurements of Zn–Al layered double hydroxide with anionic nitrate ions. *Solid State Sci* 14: 1196–1202.
11. Ahmed AAA, Talib ZA, Hussein MZB (2012) Thermal, optical and dielectric properties of Zn–Al layered double hydroxide. *Appl Clay Sci* 56: 68–76.
12. Chitrakar R, Tezuka S, Sonoda A, et al. (2008) A New Method for Synthesis of Mg–Al, Mg–Fe, and Zn–Al Layered Double Hydroxides and Their Uptake Properties of Bromide Ion. *Ind Eng Chem Res* 47: 4905–4908.
13. Seftel EM, Popovici E, Mertens M, et al. (2008) Zn–Al layered double hydroxides: Synthesis, characterization and photocatalytic application. *Micropor Mesopor Mat* 113: 296–304.
14. Marotti RE, Guerra DN, Bello C, et al. (2004) Bandgap energy tuning of electrochemically grown ZnO thin films by thickness and electrodeposition potential. *Sol Energ Mat Sol C* 82: 85–103.
15. Hussein MZB, Yun-Hin TY, Tawang MMB, et al. (2002) Thermal degradation of (zinc-aluminium-layered double hydroxide-dioctyl sulphosuccinate) nanocomposite. *Mater Chem Phys* 74: 265–271.
16. Jonscher AK (1983) *Dielectric relaxation in solids*, London: Chelsea Dielectrics Press.
17. Mehrotra V (1992) Intercalation of Layered Silicates, Layered Double Hydroxides, and Lead Iodide: Synthesis, Characterization and Properties [PhD's Dissertation], New York: Cornell University.
18. Jung H, Ohashi H, Anilkumar GM, et al. (2013) Zn^{2+} substitution effects in layered double hydroxide $(Mg_{(1-x)}Zn_x)_2Al$: textural properties, water content and ionic conductivity. *J Mater Chem A* 1: 13348–13356.
19. Furukawa Y, Tadanaga K, Hayashi A, et al. (2011) Evaluation of ionic conductivity for Mg–Al layered double hydroxide intercalated with inorganic anions. *Solid State Ionics* 192: 185–187.
20. Kim HS, Yamazaki Y, Kim JD, et al. (2010) High ionic conductivity of Mg–Al layered double hydroxides at intermediate temperature (100–200 ℃) under saturated humidity condition (100% RH). *Solid State Ionics* 181: 883–888.
21. Light TS, Licht S, Bevilacqua AC, et al. (2005) The fundamental conductivity and resistivity of water. *Electrochem Solid-State Lett* 8: E16–E19.
22. Ahmed AAA, Abidin Talib Z, Hussein MZB (2012) ESR spectra and thermal diffusivity of Zn–Al layered double hydroxide. *J Phys Chem Solids* 73: 124–128.
23. Babu KS, Chiranjivi T (1982) DC ionic conductivity in single crystals of lead nitrate. *Solid State Ionics* 6: 155–157.
24. Tripathi R, Kumar A, Bharti C, et al. (2010) Dielectric relaxation of ZnO nanostructure synthesized by soft chemical method. *Curr Appl Phys* 10: 676–681.

25. Jonscher AK (1996) *Universal relaxation law*, London: Chelsea Dielectrics Press.
26. Tripathi R, Kumar A, Bharti C, et al. (2010) Dielectric relaxation of ZnO nanostructure synthesized by soft chemical method. *Curr Appl Phys* 10: 676–681.

AIMS Press